XL CILAMCE
IBERO-LATIN AMERICAN CONGRESS ON COMPUTATIONAL METHODS IN ENGINEERING
NOVEMBER 11-14, 2019
Praiamar Natal Hotel & Convention
Natal, RN-BRAZIL

NONLINEAR POSITIONAL FORMULATION APPLIED FOR DYNAMIC 2D SOLIDS ANALYSIS CONSIDERING DIFFERENT TEMPORAL INTEGRATION METHODS

Marcos D. F. S. Saraiva
marcosdaian@hotmail.com
Dept. of Civil Engineering, Federal University of Rio Grande do Norte
Lagoa Nova, Natal, 59078-900, Rio Grande do Norte, Brazil
Daniel N. Maciel
Rodrigo Barros
dnmaciel@ect.ufrn.br
barroscivil@gmail.com
School of Sciences and Technology, Federal University of Rio Grande do Norte
Lagoa Nova, Natal, 59078-900, Rio Grande do Norte, Brazil

Abstract. The analytical resolution for dynamic problems employs partial derivarives regarding time and space. However, sereral methods of temporal integration replace the resolution of it. Thus, this paper aims to analyze the dynamic response of two dimensional structural solids through different methods of temporal integration for both implicit and explicit cases. In this sense, methods of Newmark, Houbolt and Wilson-θ are used as the implicit one. In addition, methods of Central Differences, Souza and Moura and Chung and Lee correspond to the explicit case. The analysis of 2D solids under dynamic response considers both geometric and material nonlinearities. In order to regard nonlinear geometric effect, the positional Finite Element Method (FEM) formulation wich uses node coordinates as variables instead of displacements is taken into account. Therefore, the development of each computational routines for the proposed formulation induces numerical results that are discussed and compared with examples from the specialized literature.

Keywords: Positional Finite Element Method, 2D Solids, Methods of Temporal Integration

1 Introduction

This paper aims to analyze the mechanical behavior of two dimensional structures taking into account geometric nonlinearity through Positional Finite Element Method application whose description is based on total Lagrangian formulation. This formulation shows a simple language corresponding to nonlinear geometric approach where the main advantage is the absence of co-rotational axes, where only positions are used as nodal parameters instead of displacements. This formulation can be found in several studies [1–6].

The solution of the dynamic problem makes use of temporal integration, as a result of the dynamic equilibrium equations that are represented by partial derivatives according to time and space. Hence, according to Bottura [7], one seeks to apply established numerical methodologies concerning to temporal integration, in which finite and approximate expressions are implemented from known displacements and their derivatives at a given past time t, and thus, to estimate sequential values with the purpose of obtain the dynamical equilibrium for a new time step $t + \Delta t$.

Time integration procedures can be classified into two groups, the explicit and implicit algorithms. Solutions that are achieved through the use of variables obtained by past time steps compose the group of explicit algorithms. On the other hand, implicit algorithms use variables not only associated with the past, but also relative to the current time step $t + \Delta t$.

The algorithms of temporal integration are also classified according to its stability. In general, they can be classified as stable, which present convergence in the results, and unstable, when one verifies an increasing propagation of errors over time.

The stable methods are classified as conditional and unconditional ones. As reported by Silveira [8], all explicit algorithms of temporal integration are conditionally stable. Vieira [9] says that the algorithm stability condition has a restriction on the value of the maximum time step duration adopted in each analysis.

In this context, in order to establish the stability of the explicit algorithm, it is necessary rigorous restrictions concerning to the size of the time increment value, conducting to a high computational cost in determining a quite simple problem response when compared to the performance obtained by implicit algorithms.

In accordance with Silva [10], this problem is due to the critical value for Δt is inversely proportional to the maximum natural frequency of the system, regardless the type of solicitation that a solid is submitted. Therefore, according to Vieira [9], in structural dynamics problems, whose frequencies of excitation correspond to lower natural ones, explicit methods become inefficient because the critic time step duration is lower than necessary for an accurate integration of the requested modes.

Another important consideration corresponding to explicit time integration algorithms is how the structural disposition has been discretized, due to discrepancies in the size of the elements or even different materials in the same structure, increasing, in this sense, the computational cost considerably, whereas time step duration is considered equal to all mesh, as reported by Silveira [8] and Dokainish & Subbaraj [11].

In the case of implicit methods, they are usually considered unconditionally stable, implying no restriction on the size of the time step duration, where the time interval is determined only considering the accuracy of the response desired, but not by stability of the algorithm, in agreement with Cavalcante [12]. However, traditionally, the use of implicit algorithms requires more memory for data storage during analysis, considering that it is necessary to assemble global matrix of the structural system. Thus, the implementation of implicit time integration algorithms is more complicated when compared to explicit ones as stated in Silva [10].

In general, explicit procedures are more suitable for solving problems with wave propagation, while implicit schemes are more effective for inertial problems as per Cook *et al.* [13].

Thus, the adoption of the optimal time integration algorithm for the problem studied has its difficulty related to the rapport of robustness, precision and stability according to Tamma *et al.* [14] and Cavalcante [12]. Therefore, the robustness of the algorithm is associated with its ability to generate solutions that minimize the numerical error inherent in the integration process.

Associated with problems involving inertial forces, several models have been improved over time, especially in the field of numerical methods. Hence, in this paper, the temporal discretization will be performed in different explicit and implicit temporal integration algorithms in order to verify the nonlinear physical and geometric behavior in different propositions.

2 Positional numerical method

The total mechanical energy functional for dynamic problems is determined by four terms of energy, represented by total strain energy U_e, the potential energy of applied force P, kinetic energy K_c and dissipation energy due to mechanical system damping K_a, as descripted in Eq. (1):

$$\Pi = U_e + K_c + K_a - P. \quad (1)$$

Applying the minimum potential energy principle, the position established to the dynamic equilibrium can be defined in each time t, in the initial volume V_0

$$\left.\frac{\partial \Pi}{\partial X_s}\right|_t = \int_{V_0} \frac{\partial u_e(\xi,\eta,X_i)}{\partial X_s} dV_0 + \int_{V_0} \rho_0 \dot{x}_i(\xi,\eta,X_i) \frac{\partial \dot{x}_i(\xi,\eta,X_i)}{\partial X_s} dV_0 - F_s + \int_{V_0} c_m \rho_0 \dot{x}_i(\xi,\eta,X_i) dV_0 = 0. \quad (2)$$

Where u_e is the specific strain energy, ρ_0 is the density of the body, $\dot{x}_i$ is the vector of velocity, q represents the specific dissipative energy functional and c_m is the damping coefficient. ξ and η are non-dimensional Hammer coordinates.

Considering index notation, for the current time step $(t + \Delta t)$, the Eq. (2) is rewritten as:

$$\left.\frac{\partial \Pi}{\partial X}\right|_{t+\Delta t} = \left.\frac{\partial U_e}{\partial x_s}\right|_{t+\Delta t} - F_{t+\Delta t} + M\ddot{X}_{t+\Delta t} + C\dot{X}_{t+\Delta t} = 0. \quad (3)$$

Where M is the mass matrix, C is the damping matrix and external forces are represented by F. The term $\partial U_e / \partial x_s$ characterizes the material nonlinearity. The elastic strain is obtained according to Eq. (4), based on total strain and its correspondent plastic portion

$$\varepsilon_{ij}^{e} = \varepsilon_{ij} - \varepsilon_{ij}^{p}. \quad (4)$$

Hence, the stress tensor can be represented in function of the plastic strain, as descripted on Eq. (5), where C^{ep} is the consistent tangent operator.

$$\sigma_{ij} = C_{ijkl}\varepsilon_{kl}^{e} = C_{ijkl}^{ep}(\varepsilon_{ij} - \varepsilon_{ij}^{p}). \quad (5)$$

The vector of internal forces $\partial U_e / \partial x_s$, is determined by volumetric integration of specific strain energy derivative regarding the position, showing the term of plastic strain, as follows:

$$\frac{\partial U_e}{\partial X_s} = \int_{V_0} \frac{\partial u_e}{\partial X_s} dV_0 = \int_{V_0} \frac{1}{2}\frac{\partial}{\partial X_s}(\sigma_{kl}\varepsilon_{mn}^{e}) dV_0 = \int_{V_0} \frac{1}{2}\frac{\partial}{\partial X_s}\left(\varepsilon_{kl}^{e} C_{klmn}^{ep} \varepsilon_{mn}^{e}\right) dV_0. \quad (6)$$

In order to solve the sistem achieved on Eq. (3), Newton-Raphson procedure [2] is applied for the current time step $(t + \Delta t)$. Furthermore the temporal integration methods are considered as an alternative concerned to the time integration resolution.

Therefore, six temporal integration algorithms, Newmark, Houbolt, Wilson-θ, Souza & Moura [15], Central Differences and Chung & Lee [16], will be described in order to adjust to the positional formulation, where each algorithm is characterized by the particular equations of position, velocity and acceleration, implying in dynamic equilibrium modified equations.

2.1 Implicit Method of Newmark

The Method of Newmark is one of the most widespread in the literature, and it has large application in structural problems. The method was developed in 1959 by Newmark, wherein he presented the single step method as indicated in Eq. (7) and Eq. (8), representing, respectively, the approximate position and velocity.

$$X_{t+\Delta t} = X_t + \Delta t\dot{X}_t + \Delta t^2 \left[\left(\frac{1}{2} - \beta\right)\ddot{X}_t + \beta\ddot{X}_{t+\Delta t}\right]. \quad (7)$$

$$\dot{X}_{t+\Delta t} = \dot{X}_{t+\Delta t} + \Delta t(1-\gamma)\ddot{X}_{t+\Delta t} + \gamma\Delta t\ddot{X}_{t+\Delta t}. \quad (8)$$

The β e γ parameters are so-called Newmark coefficients and they determine the proprieties of stability, precision and damping as discussed by Cook *et al.* [13]. These coefficients, according to Bottura [7], consider how implicit the method is. For null values for its parameters, the algorithm assumes explicit characteristics.

In line with Hughes [17], the method of Newmark is unconditionally stable for $1/2 \leq \gamma \leq 2\beta$ and conditionally stable for $\gamma \leq 1/2$ and $\beta \leq \gamma/2$.

Manipulating the Eq. (7), we obtain the acceleration for the current time step:

$$\ddot{X}_{t+\Delta t} = \frac{X_{t+\Delta t} - X_t}{\beta\Delta t^2} - \frac{\dot{X}_t}{\beta\Delta t} - \left(\frac{1}{2} - \beta\right)\ddot{X}_t. \quad (9)$$

Applying Eq. (8) and Eq. (9) in Eq. (3):

$$\left.\frac{\partial\Pi}{\partial X}\right|_{t+\Delta t} = \left.\frac{\partial U_e}{\partial X}\right|_{t+\Delta t} - F_{t+\Delta t} + \frac{M}{\beta\Delta t^2}X_{t+\Delta t} - MQ_t + CR_t + \frac{\gamma C}{\beta\Delta t}X_{t+\Delta t} - \gamma\Delta tCQ_t = 0. \quad (10)$$

The dynamic contribution of variables in the last time step (t), is represented by Q_t and R_t, expressed respectively on Eq. (11) and Eq. (12):

$$Q_t = \frac{X_t}{\beta\Delta t^2} + \frac{\dot{X}_t}{\beta\Delta t} + \left(\frac{1}{2} - \beta\right)\ddot{X}_t. \quad (11)$$

$$R_t = \dot{X}_t + \Delta t(1-\gamma)\ddot{X}_t. \quad (12)$$

The Hessian Matrix ($\nabla g(X_0)$) is determined from second order derivative of the total mechanical energy functional regarding nodal positions, in consonance with Silva [10].

$$\nabla g(X_0) = \frac{\partial^2\Pi}{\partial X^2}. \quad (13)$$

Applying the second derivative in Eq. (10) regarding nodal positions for the current time step ($t + \Delta t$), we obtain the Hessian Matrix for the dynamic problem, as follows:

$$\left.\frac{\partial^2\Pi}{\partial X^2}\right|_{t+\Delta t} = \nabla g(X_0) = \left.\frac{\partial^2 U_e}{\partial X^2}\right|_{t+\Delta t} + \frac{M}{\beta\Delta t^2} + \frac{\gamma C}{\beta\Delta t}. \quad (14)$$

2.2 Implicit method of Houbolt

Houbolt [18] presented a temporal integration method whose variables of velocity and acceleration are determined by expressions in descent finite differences, corresponding to a multiple pass method, conforming to Bottura [7]. It is an unconditionally stable method resulted from the second order derivation of Lagrange cubic polynomials regarding the time, as per Bathe [19].

Hence, acceleration and velocity are described, respectively as follows:

$$\ddot{X}_{t+\Delta t} = \frac{1}{\Delta t^2}(2X_{t+\Delta t} - 5X_t + 4X_{t-\Delta t} - X_{t-2\Delta t}). \quad (15)$$

$$\dot{X}_{t+\Delta t} = \frac{1}{6\Delta t}(11X_{t+\Delta t} - 18X_t + 9X_{t-\Delta t} - 2X_{t-2\Delta t}). \quad (16)$$

Applying Eq. (15) and Eq. (16) into Eq. (3) that defines the dynamic equilibrium for the current time step ($t + \Delta t$), we obtain:

$$\left.\frac{\partial\Pi}{\partial X}\right|_{t+\Delta t} = \left.\frac{\partial U_e}{\partial X}\right|_{t+\Delta t} - F_{t+\Delta t} + \frac{2M}{\Delta t^2}X_{t+\Delta t} + MQ_t + \frac{11C}{6\Delta t}X_{t+\Delta t} + CR_t = 0. \quad (17)$$

Where:

$$Q_{\mathrm{t}} = \frac{1}{\Delta t^2}(-5X_t + 4X_{t-\Delta\mathrm{t}} - X_{t-2\Delta\mathrm{t}}). \quad (18)$$

$$R_{\mathrm{t}} = \frac{1}{6\Delta t}(-18X_t + 9X_{t-\Delta\mathrm{t}} - 2X_{t-2\Delta\mathrm{t}}). \quad (19)$$

The Hessian Matrix for the dynamic problem is achieved from the derivative of Eq. (17) regarding nodal positions for the current time step, as follows:

$$\left.\frac{\partial^2\Pi}{\partial X^2}\right|_{t+\Delta t} = \nabla g(X_0) = \left.\frac{\partial^2 U_e}{\partial X^2}\right|_{t+\Delta t} + \frac{2M}{\Delta t^2} + \frac{11C}{6\Delta t}. \tag{20}$$

2.3 Implicit method of Wilson-θ

Wilson & Bathe [20] presented a modification of the linear acceleration method in order to become it in a unconditionally stable method through the incorporation of the factor θ_w, because the unstable solution tends to oscillate around the truth solution.as discussed by Wilson [21].

The method of Wilson-θ considers acceleration as a linear variable in a time interval between t and $\theta_w\Delta t$. Thus, this problem is solved for a time step concerned to $t + \theta_w\Delta t$.

The factor θ_w must assume value greater or equal to 1. If equal 1, the method of Newmark do not modifies. If greater than 1.37, this method becomes unconditionally stable. According to Craig Jr. [22], the optimal value for θ_w is 1.420815, but employed 1.4 by several other authors.

Assuming an increment in time τ as that $0 \le \tau \le \theta_w\Delta t$, for the time interval between t and $t+\theta_w\Delta t$, the acceleration is described as:

$$\ddot{X}_{t+\tau} = \ddot{X}_t + \frac{\tau}{\theta_w\Delta t}\left(\ddot{X}_{t+\theta_w\Delta t} - \ddot{X}_t\right). \tag{21}$$

The velocity and position are determined via integration from Eq. (21):

$$\dot{X}_{t+\tau} = \dot{X}_t + \ddot{X}_t\tau + \frac{\tau^2}{2\theta_w\Delta t}\left(\ddot{X}_{t+\theta_w\Delta t} - \ddot{X}_t\right). \tag{22}$$

$$X_{t+\tau} = X_t + \dot{X}_t\tau + \frac{\ddot{X}_t\tau^2}{2} + \frac{\tau^3}{6\theta_w\Delta t}\left(\ddot{X}_{t+\theta_w\Delta t} - \ddot{X}_t\right). \tag{23}$$

Considering $\tau = \theta_w\Delta t$, the Eq. (22) and Eq. (23) are rewritten as:

$$\dot{X}_{t+\theta_w\Delta t} = \dot{X}_t + \frac{\theta_w\Delta t}{2}\left(\ddot{X}_{t+\theta_w\Delta t} + \ddot{X}_t\right). \tag{24}$$

$$X_{t+\theta_w\Delta t} = X_t + \theta_w\Delta t\dot{X}_t + \frac{{\theta_w}^2\Delta t^2}{6}\left(\ddot{X}_{t+\theta_w\Delta t} + 2\ddot{X}_t\right). \tag{25}$$

Hence, we determine the corresponding equations for $\dot{X}_{t+\theta_w\Delta t}$ and $\ddot{X}_{t+\theta_w\Delta t}$ in terms of $X_{t+\theta_w\Delta t}$, from Eq. (24) and Eq. (25), as follows:

$$\ddot{X}_{t+\theta_w\Delta t} = \frac{6}{{\theta_w}^2\Delta t^2}\left(X_{t+\theta_w\Delta t} - X_t\right) - \frac{6}{\theta_w\Delta t}\dot{X}_t - 2\ddot{X}_t. \tag{26}$$

$$\dot{X}_{t+\theta_w\Delta t} = \frac{3}{\theta_w\Delta t}\left(X_{t+\theta_w\Delta t} - X_t\right) - 2\dot{X}_t - \frac{\theta_w\Delta t}{2}\ddot{X}_t. \tag{27}$$

Positions, velocities and accelerations concerned to the current time step $t + \Delta t$ are determined through the instant $t + \theta_w\Delta t$. Similarly, the vector of external forces is estimated for $t + \theta_w\Delta t$ as follows:

$$F_{t+\theta_w\Delta t} = F_t + \theta_w(F_{t+\Delta t} - F_t). \tag{28}$$

Based on Eq. (26) and Eq. (27), the Eq. (3) is determined, for $t + \theta_w\Delta t$, as:

$$\left.\frac{\partial\Pi}{\partial X}\right|_{t+\theta_w\Delta t} = \left.\frac{\partial U_e}{\partial X}\right|_{t+\theta_w\Delta t} - F_{t+\theta_w\Delta t} + \frac{6M}{{\theta_w}^2\Delta t^2}X_{t+\theta_w\Delta t} + MQ_t + \frac{3C}{\theta_w\Delta t}X_{t+\theta_w\Delta t} + CR_t = 0. \tag{29}$$

Where:

$$Q_t = -\left(\frac{6}{{\theta_w}^2\Delta t^2}X_t + \frac{6}{\theta_w\Delta t}\dot{X}_t + 2\ddot{X}_t\right). \tag{30}$$

$$R_t = -\left(\frac{3}{\theta_w\Delta t}X_t + 2\dot{X}_t + \frac{\theta_w\Delta t}{2}\ddot{X}_t\right). \tag{31}$$

The Hessian matrix is achieved through Eq. (29):

$$\left.\frac{\partial^2\Pi}{\partial X^2}\right|_{t+\theta_w\Delta t} = \nabla g(X_0) = \left.\frac{\partial^2 U_e}{\partial X^2}\right|_{t+\theta_w\Delta t} + \frac{6M}{{\theta_w}^2\Delta t^2} + \frac{3C}{\theta_w\Delta t}. \tag{32}$$

In order to apply the current time step $t + \Delta t$, we consider $\tau = \Delta t$ in Eq. (21), Eq. (22) and Eq. (23). Therefore:

$$\ddot{X}_{t+\Delta t} = \ddot{X}_t + \frac{1}{\theta_w}\left(\ddot{X}_{t+\theta_w \Delta t} - \ddot{X}_t\right). \tag{33}$$

$$\dot{X}_{t+\Delta t} = \dot{X}_t + \Delta t \ddot{X}_t + \frac{\Delta t}{2\theta_w}\left(\ddot{X}_{t+\theta_w \Delta t} - \ddot{X}_t\right). \tag{34}$$

$$X_{t+\Delta t} = X_t + \Delta t \dot{X}_t + \frac{\Delta t^2}{2}\ddot{X}_{\mathrm{t}} + \frac{\Delta t^2}{6\theta_w}\left(\ddot{X}_{t+\theta_w \Delta t} + 2\ddot{X}_t\right). \tag{35}$$

2.4 Explicit method of Central Differences

According to Silva [10], the method of Central Differences is a particularization from Newmark method, where $\beta = 0$, exhibiting second order accuracy. Cook *et al.* [13] considers that acceleration and velocity are attained by central differences approach.

Among the explicit methods, this is one of the most employed, mainly regarding dynamic problems. However, small time increments are indispensable, because of the conditionally stable characteristic.

In this sense, the positions $X_{t-\Delta t}$ and $X_{t+\Delta t}$, are descripted by Taylor expansion centered in X_t, as follows:

$$X_{t+\Delta t} = X_t + \Delta t \dot{X}_t + \frac{\Delta t^2}{2}\ddot{X}_t + \cdots. \tag{36}$$

$$X_{t-\Delta t} = X_t - \Delta t \dot{X}_t + \frac{\Delta t^2}{2}\ddot{X}_t - \cdots. \tag{37}$$

The truncated sum under the terms of the second order produces:

$$\ddot{X}_t = \frac{1}{\Delta t^2}\left(X_{t+\Delta t} - 2X_t + X_{t-\Delta t}\right). \tag{38}$$

Analogously, the difference between Eq. (36) and Eq. (37) determines:

$$\dot{X}_t = \frac{1}{2\Delta t}\left(X_{t+\Delta t} - X_{t-\Delta t}\right). \tag{39}$$

Applying Eq. (38) and Eq. (39) into Eq. (3), we obtain:

$$\left.\frac{\partial \Pi}{\partial X}\right|_{t+\Delta t} = \left.\frac{\partial U_e}{\partial X}\right|_{t+\Delta t} - F_{t+\Delta t} + \frac{M}{\Delta t^2}X_{t+\Delta t} + MQ_t + \frac{C}{2\Delta t}X_{t+\Delta t} + CR_t = 0. \tag{40}$$

Where:

$$Q_{\mathrm{t}} = -2X_t + X_{t-\Delta \mathrm{t}}. \tag{41}$$

$$R_{\mathrm{t}} = -X_{t-\Delta \mathrm{t}}. \tag{42}$$

From Eq. (40), one has the Hessian Matrix:

$$\left.\frac{\partial^2 \Pi}{\partial X^2}\right|_{t+\Delta t} = \nabla g(X_0) = \left.\frac{\partial^2 U_e}{\partial X^2}\right|_{t+\Delta t} + \frac{M}{\Delta t^2} + \frac{C}{2\Delta t}. \tag{43}$$

For the purpose to avoid errors propagations along times step, as presented by Bathe [19], the increment of time must be smaller than a critical value:

$$\Delta t_{crit} \leq \frac{T_\pi}{\pi}. \tag{44}$$

Where T_π is the shortest period of the finite element system and can be estimated by Eq. (45).

$$T_\pi \leq \frac{2\pi}{\omega_{max}}. \tag{45}$$

Where ω_{max} is the largest natural frequency.

2.5 Explicit method of Souza & Moura [15]

Souza & Moura [15] produced a method with the purpose of decrease possible errors that are achieved through the use of the Central Differences method, especially when adopting a time increment close to the critical value. This methodology, while retaining the advantages of an explicit method, essentially eliminates spurious numerical oscillations.

The main purpose of this method is describe the velocity and acceleration as a Lagrangian Polynomial of four degrees. Thus:

$$\dot{X}_t = \frac{1}{2\Delta t}(X_{t+\Delta t} - X_{t-\Delta t}) - \frac{1}{12\Delta t}(X_{t-3\Delta t} - 6X_{t-2\Delta t} + 12X_{t-\Delta t} - 10X_t + 3X_{t+\Delta t}). \quad (46)$$

$$\ddot{X}_t = \frac{1}{\Delta t^2}(X_{t+\Delta t} - 2X_t + X_{t-\Delta t}) - \frac{1}{12\Delta t^2}(X_{t+\Delta t} - 4X_t + 6X_{t-\Delta t} - 4X_{t-2\Delta t} + X_{t-3\Delta t}). \quad (47)$$

Applying Eq. (46) and Eq. (47) into Eq. (3), one has:

$$\left.\frac{\partial \Pi}{\partial X}\right|_{t+\Delta t} = \left.\frac{\partial U_e}{\partial X}\right|_{t+\Delta t} - F_{t+\Delta t} + \frac{11M}{12\Delta t^2}X_{t+\Delta t} + MQ_t + \frac{C}{4\Delta t}X_{t+\Delta t} + CR_t = 0. \quad (48)$$

Where:

$$Q_{\mathrm{t}} = \frac{1}{12\Delta t^2}(-20X_t + 6X_{t-\Delta t} + 4X_{t-2\Delta t} - X_{t-3\Delta t}). \quad (49)$$

$$R_{\mathrm{t}} = \frac{1}{12\Delta t}(-X_{t-3\Delta t} + 6X_{t-2\Delta t} - 18X_{t-\Delta t} + 10X_t). \quad (50)$$

The Hessian Matrix is given by:

$$\left.\frac{\partial^2 \Pi}{\partial X^2}\right|_{t+\Delta t} = \nabla g(X_0) = \left.\frac{\partial^2 U_e}{\partial X^2}\right|_{t+\Delta t} + \frac{11M}{12\Delta t^2} + \frac{C}{4\Delta t}. \quad (51)$$

With the intention of acquire stability, the increment of time is written as follows:

$$\Delta t_{crit} \leq \sqrt{\frac{2}{3}}\frac{2}{\omega_{max}}. \quad (52)$$

2.6 Explicit method of Chung & Lee [16]

Chung & Lee [16] proposed a new family of second order temporal integration algorithms with high frequency dissipation for several dynamic problems. Positions and velocities are given by:

$$X_{t+\Delta t} = X_t + \Delta t\dot{X}_t + \beta_1\ddot{X}_t + \beta_2\ddot{X}_{t+\Delta t}. \quad (53)$$

$$\dot{X}_{t+\Delta t} = \dot{X}_t + \Delta t\dot{X}_t + \gamma_1\ddot{X}_t + \gamma_2\ddot{X}_{t+\Delta t}. \quad (54)$$

Where:

$$\beta_1 = \Delta t^2\left(\frac{1}{2} - \beta_c\right). \quad (55)$$

$$\beta_2 = \Delta t^2\beta_c. \quad (56)$$

$$\gamma_1 = -\frac{1}{2}\Delta t. \quad (57)$$

$$\gamma_2 = \frac{3}{2}\Delta t. \quad (58)$$

Therefore, the proposed method presents only a free parameter, corresponding to β_c. From a study of accuracy, stability and convergence, one has:

$$1 \leq \beta_c \leq \frac{28}{27}. \quad (59)$$

The current acceleration is given by:

$$\ddot{X}_{t+\Delta t} = \frac{(X_{t+\Delta t} - X_t)}{\beta_2} - \frac{\Delta t\dot{X}_t}{\beta_2} - \frac{\beta_1\ddot{X}_t}{\beta_2}. \quad (60)$$

Applying Eq. (54) and Eq. (60) into Eq. (3), one has:

$$\left.\frac{\partial \Pi}{\partial X}\right|_{t+\Delta t} = \left.\frac{\partial U_e}{\partial X}\right|_{t+\Delta t} - F_{t+\Delta t} + \frac{M}{\beta_2} X_{t+\Delta t} + M Q_t + \frac{\gamma_2 C}{\beta_2} X_{t+\Delta t} + C R_t = 0. \tag{61}$$

Where:

$$Q_t = -\frac{X_t}{\beta_2} - \frac{\Delta t \dot{X}_t}{\beta_2} - \frac{\beta_1 \ddot{X}_t}{\beta_2}. \tag{62}$$

$$R_t = \dot{X}_t + \Delta t \dot{X}_t + \gamma_1 \ddot{X}_t + \gamma_2 Q_t. \tag{63}$$

The Hessian Matrix is given by:

$$\left.\frac{\partial^2 \Pi}{\partial X^2}\right|_{t+\Delta t} = \nabla g(X_0) = \left.\frac{\partial^2 U_e}{\partial X^2}\right|_{t+\Delta t} + \frac{M}{\beta_2} + \frac{\gamma_2 C}{\beta_2}. \tag{64}$$

The method of Chung & Lee [16], when $\beta_c = 1$, presents similar characteristics with Central Differences one. However, for values close to the upper limit of 28/27, the method has maximum numerical dissipation.

3 Numerical examples

A set of examples found in the specialized literature are performed herein with the purpose of compare the dynamic response obtained by several methods of temporal integration. For this, the adopted parameters are given by: $\gamma = 0{,}5$, $\beta = 0{,}25$, $\theta_w = 1{,}420815$, $\beta_c = 1{,}03$.

In this paper, the formulation is composed by two degrees of freedom by node and constant thickness is considered. Moreover, triangular finite element with cubic approximation is adopted.

3.1 Undamped Cantilever beam

In this example, found in Greco [23] as well as Marques [24] and Maciel [25], a robust cantilever beam is subjected to an impact loading at the free end, as shown in Fig. 1.

The purpose of this example is to verify the behavior of the several temporal integration algorithms adopted in this paper. Therefore, the beam is discretized by 88 two-dimensional finite elements with two different time steps of $0{,}0001s$ and $0{,}00001s$, respectively for the first and second responses, in order to verify the influence of this parameter in different temporal integration methods adopted. Two models of loading are adopted. The first one considers a constant loading. The second model admits an increase loading until a given time beyond which it becomes constant.

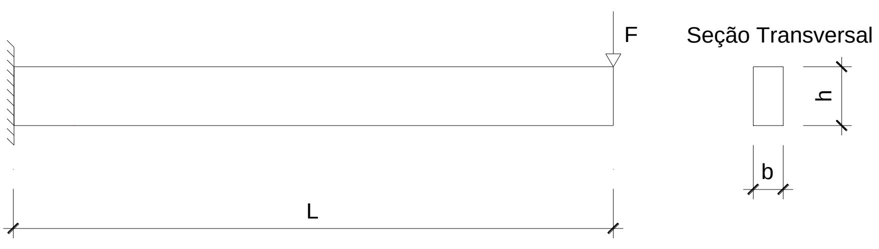

Figure 1 – Cantilever beam scheme

The mechanical and geometrical proprieties are given by:

$E = 210\ 10^9 N/m^2$ $\nu = 0$
$L = 1200mm$ $b = 150mm$
$h = 300mm$ $\rho = 1691{,}81\ 10^{-4}\ N\ s^2/m^4$

The first providence in determining temporal integration, in accordance with Bathe & Wilson [20], corresponds to setting the appropriate value for the time interval, because it is directly related to the truth structure behavior and numerical instability problems. In this context, Fig. 2 and Fig. 3, as well as Fig. 4 and Fig. 5 compare the displacement of the node where the loading is applied, adopting several time integration methods with different time intervals.

It is possible to see in Fig. 2 and Fig. 3 the influence of the time factor on the structural response, especially for the explicit methods. Due to the decrease of time interval, the behavior of the responses from different methods of temporal integration tend to assume the same form.

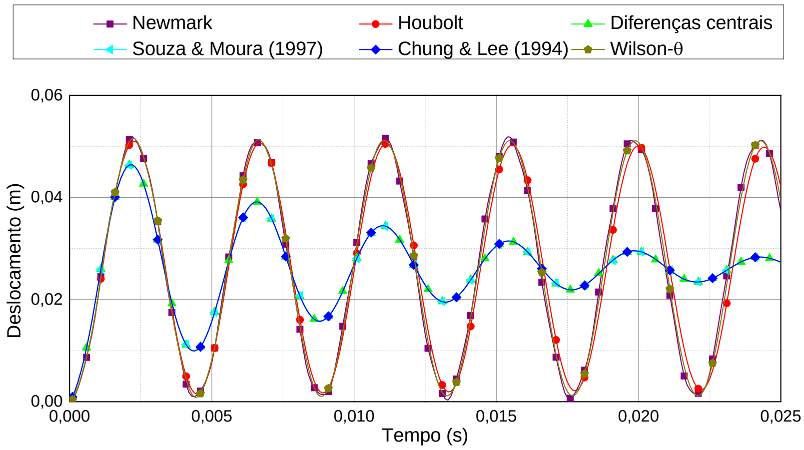

Figure 2 – Case 1 discretized for $\boldsymbol{\Delta t = 0,0001\ s}$.

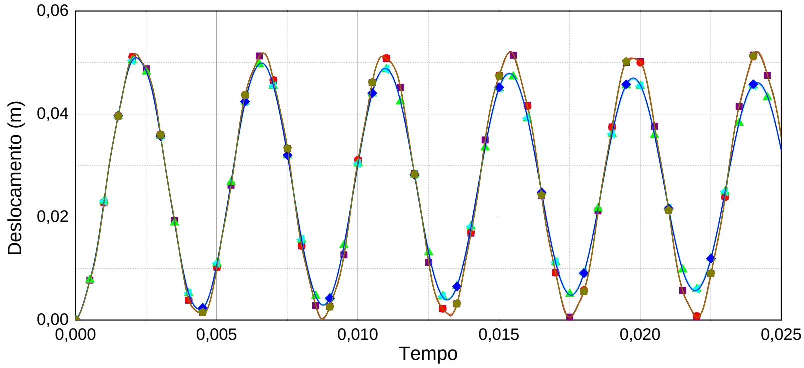

Figure 3 – Case 1 discretized for $\boldsymbol{\Delta t = 0,00001\ s}$.

Figures 2 and 4 shows a small difference between the results obtained by explicit methods. As discussed by Cavalcante [12], the method of Chung & Lee [16] exhibited a small numerical damping, when compared with Souza & Moura [15] and Central Differences ones, depending of β_c.

It is perceived a certain damping dissipation presented by the explicit methods when compared to the implicit ones, mainly for fairly greater time intervals. As its decreasing, the energy dissipation of explicit methods is reduced, whereas the implicit methods do not experiment important changes.

The method of Newmark expounded results almost identical to those obtained in the literature, regardless time interval analyzed. The methods of Houbolt and Wilson-θ show a feeble damping that is reduced with the decrease of time interval.

In general, the computational effort required by the explicit methods is smaller, however, they need a greater temporal discretization. In addition, explicit and implicit methods tend to converge to the same result as the time interval is decreased.

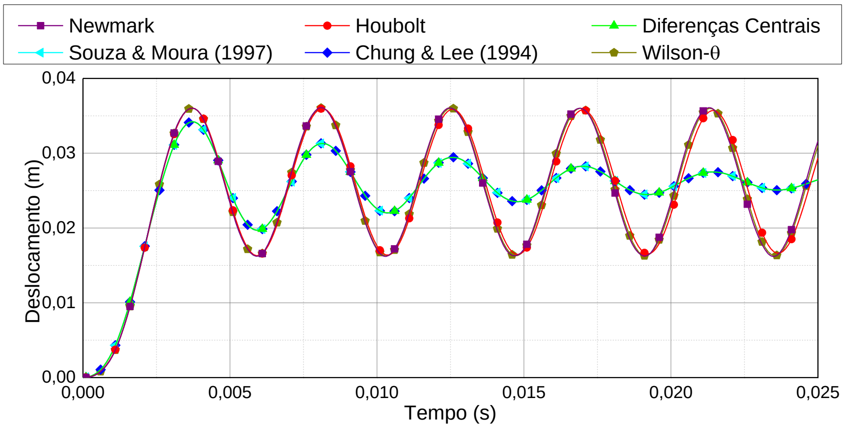

Figure 4 – Case 2 discretized for $\boldsymbol{\Delta t = 0,0001\ s}$

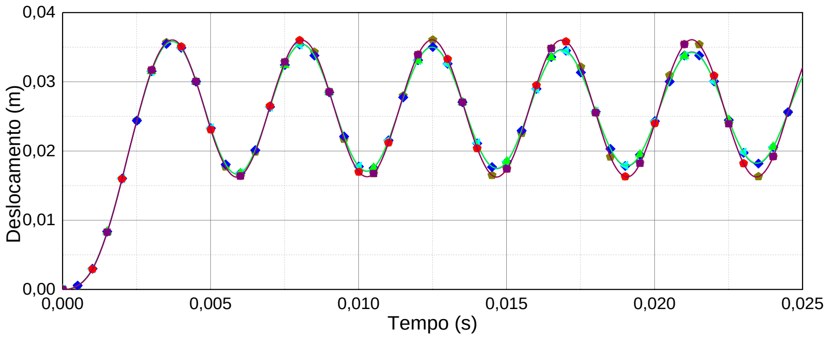

Figure 5 – Case 2 discretized for $\boldsymbol{\Delta t = 0,00001\ s}$

3.2 Rod-crank mechanism

In this example proposed by Marques [24], the performance of temporal integration algorithms applied in a rod-crank mechanism is verified. Hence, Fig. 6 shows a scheme about this mechanism which is composed by a rod and a crank, connected to each other in the point *A*. The rod is articulated in the point *C*. The crank turns around the axis placed in *B*.

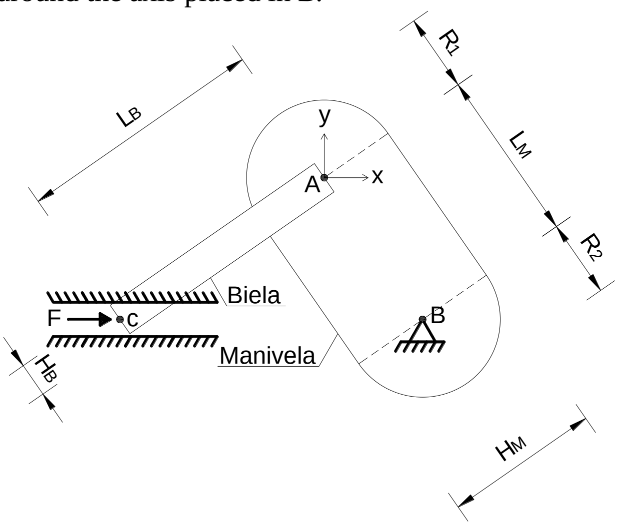

Figure 6 – Rod-crank mechanism scheme

The mechanical and geometrical proprieties are given by:

$E = 210\ 10^9 kg/cm^2$ $c_m = 5\ s^{-1}$ $\rho = 0{,}0079\ kg/cm^3$
$L_B = 14{,}4\ cm$ $H_B = 2\ cm$ $h_B = 1\ cm$
$L_M = 10{,}0\ cm$ $H_M = 9\ cm$ $h_M = 1\ cm$
$R_1 = 4{,}50\ cm$ $R_2 = 4{,}50\ cm$ $\nu = 0$

The dynamic response is obtained for two different time steps $\Delta t = 0{,}00025\ s$ and $\Delta t = 0{,}00005\ s$. The assembly is discretized by 312 finite elements. Furthermore, it is considered a load $F = 100000\ kg\ cm/s^2$ applied at point *C*. The loading occurs during a half revolution.

In accordance with Fig. 7 and Fig. 8, some structural displacements for several time step are presented, using Houbolt method. This analysis shows that the time required to perform the current cycle is lower than the one observed for the previous period until achieving a constant time of revolution.

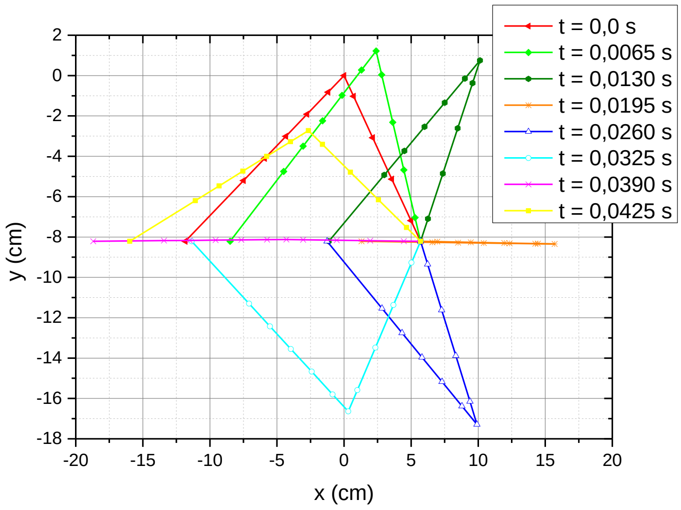

Figure 7 – Displacement for the first rotation cycle

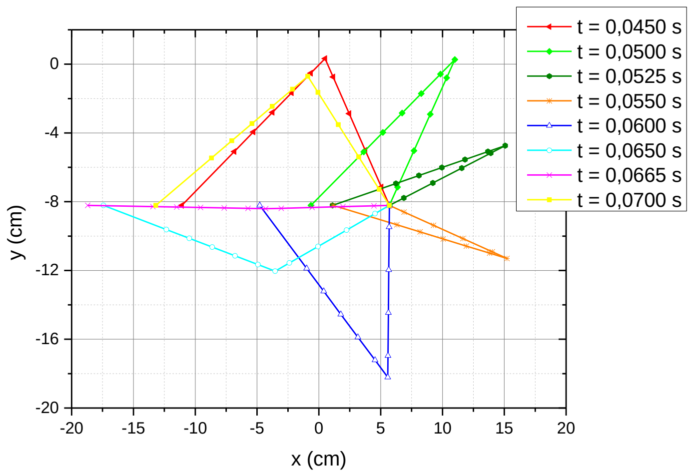

Figure 8 – Displacement for the second rotation cycle

To evaluate the performance of temporal integration algorithms in this example, the response of horizontal position for the load application point is presented. As shown in Fig. 9, a similar behavior is remarked when the discretization is performed with smaller time step.

In addition, the algorithms proposed by Souza & Moura [15] and Central Differences exhibited identical behavior for both cases, but the period of revolution performed by them is superior that one verified on implicit methods just because they are highly dissipative. The method proposed by Chung & Lee [16] proved to be ineffective in the convergence of results.

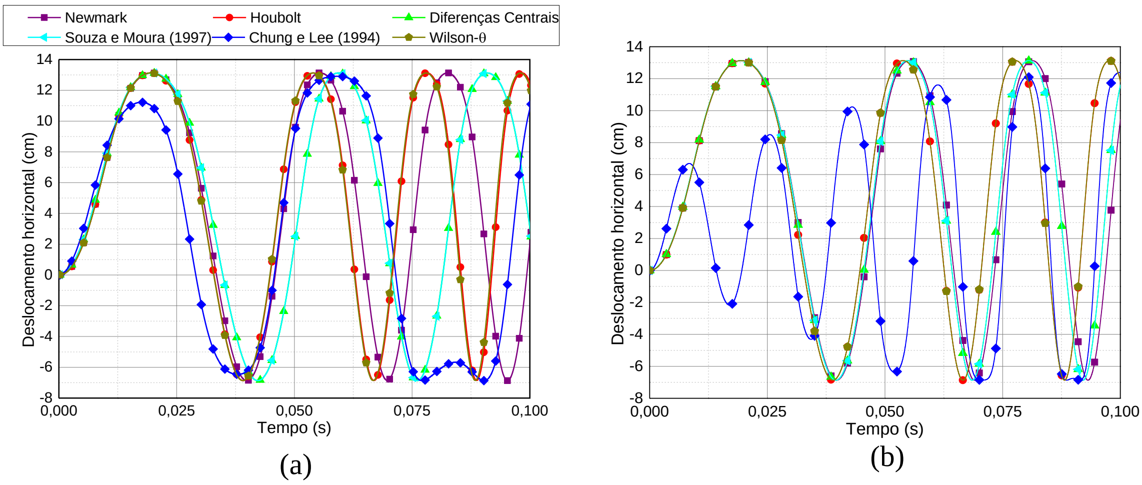

Figure 9 – Horizontal position for the load application point. a) $\boldsymbol{\Delta t = 0,00025\ s}$. b) $\boldsymbol{\Delta t = 0,00005\ s}$

Methods of Houbolt and Wilson-θ presented consistent response, showing very close results in both situations, regardless time step adopted. The method of Newmark demonstrated to converge as the time step reduces.

4 Conclusion

The main objective was to analyze the structural behavior of two-dimensional solids considering geometric and material nonlinearities. This paper contributes significatively about this theme, because it can approach the truth performance. Therefore, a positional formulation was performed by comparison with specialized literature, in order to investigate the behavior of two-dimensional structures.

The temporal integration methods applied in this paper was evaluated through several examples considering dynamic load applied in different structures. In general, explicit algorithms showed more coherent results when associated with smaller time step. However, methods of Houbolt, Wilson-θ and Newmark are more suitable in rotational cases. Due to the need for calibration, the method of Newmark is less indicated than other implicit methods. Explicit methods of Central Differences and Souza & Moura [15] exhibit certain instability that can easily be reduced by considering shorter time intervals.

Acknowledgments

The authors would like to thank the Brazilian Research Funding Agencies CAPES (Coordination of Improvement of Higher Education Personnel) and CNPq (National Council for Scientific and Technological Development) for the financial supports.

References

[1] H. B. Coda and M. Greco. Simple FEM formulation for large deflection 2D frame analysis based on position description. *Computer Methods in Applied Mechanics and Engeneering*, vol. 193, n. 33–35, pp. 3541–3557, 2004.
[2] M. Greco and H. B. Coda. Positional FEM formulation for flexible multi-body dynamic analysis. *Journal of Sound and Vibration*, vol. 290, n. 3–5, pp. 1141–1174, 2006.
[3] R. Carrazedo and H. B. Coda. Alternative positional FEM applied to thermomechanical impact of truss structures. *Finite Elements in Analysis and Design*, vol. 46, n. 11, pp. 1008–1016, 2010.

[4] H. B. Coda and R. R. Paccola. An alternative positional FEM formulation for geometrically non-linear analysis of shells: curved triangular isoparametric elements. *Computational Mechanics*, vol. 40, pp. 185–200, 2007.
[5] J. P. B. Cavalcante, D. N. Maciel, M. Greco. Impact Response of Flying Objects Modeled by Positional Finite Element Method. *International Journal of Structural Stability and Dynamics*, vol. 18, n. 6, 2018.
[6] J. P. B. Cavalcante, D. N. Maciel, M. Greco, J. N. Silva Filho. A Simple FEM Formulation Applied to Nonlinear Problems of Impact with Thermomechanical Coupling. *Latin American Journal of Solids and Structures*, vol. 14, n. 13, pp. 2439–2462, 2017.
[7] H. M. Bottura. Uma família de algoritmos hermitianos para a integração direta das equações de dinâmica das estruturas. PhD thesis, University of São Paulo, 1997.
[8] E. S. S. Silveira. Análise dinâmica de linhas de ancoragem com adaptação no tempo e subciclagem. PhD thesis, Pontifical Catholic University of Rio de Janeiro, 2001.
[9] L. C. L. M.Vieira. Estudo de algoritmos de integração elemento por elemento para análise dinâmica não linear de estruturas. MS dissertation, Federal University of Alagoas, 2004.
[10] R. L. Silva. Estudo de pórticos planos não-lineares considerando os efeitos térmicos. MS dissertation, Federal University of Rio Grande do Norte, 2017.
[11] M. A. Dokainish and K. Subbaraj. A survey of direct time-integration methods in computational structural dynamics-I Explicit methods. *Computers & Structures*, vol 32, n. 6,pp. 1371-1386, 1989.
[12] J. P. B. Cavalcante. Contribuição ao estudo de treliças não lineares considerando efeitos térmicos. MS dissertation, Federal University of Rio Grande do Norte, 2016.
[13] R. D. Cook, D. S. Malkus, M. E. Plesha. *Concepts and Applications of Finite Element Analysis*. Jonh Wiley & Sons, 1989.
[14] K. K. Tamma, X. Zhou, D. Sha. The time dimension – A theory towards the evolution, classification, characterization and design of computational algorithms for transient-dynamic applications. *Archives of Computacional Methods in engineering*, vol. 7, n. 2, pp. 67-290, 2000.
[15] L. A. S. Souza and C. A. Moura, 1997. Diferença finita de quarta ordem para integração explícita no domínio do tempo de problemas elastodinâmicos. *XVIII Ibero Latin American Congress on Computational Methods in Engineering (CILAMCE)*, pp. 767-774.
[16] J. Chung and J. M. Lee, (1994): A new family of explicit time integration methods for linear and non-linear structural dynamics. *International Journal for Numerical Methods in Engineering*, vol. 37, n. 23, pp. 3961-3976, 1994.
[17] T. J. R. Hughes. *The Finite Element Method: Linear Static and Dynamic Finite Element Analysis*. Dover Publications INC, 2000.
[18] J. C. Houbolt. A Recurrence matrix solution for the dynamic response of aircraft. *Journal of Aeronautical Sciences*, vol. 17, pp. 540-550, 1950.
[19] K. J. Bathe. *Finite Element Procedures*. Prentice Hall, 1996.
[20] E. L. Wilson and K. J. Bathe. Stability and Accuracy Analysis of Direct Integration Methods. *Earthquake Engineering and Structural Dynamics*, vol. 1, pp. 283-291, 1973.
[21] E. L. Wilson. *Three-dimensional static and dynamic analysis of structures.* Computers and Structures Inc., 2002.
[22] R. R. Craig Jr. *Structural dynamics – An introduction to computer methods*. J. Wiley,1981.
[23] M. Greco. Análise de problemas de contato/impacto em estruturas de comportamento não-linear pelo método dos elementos finitos. PhD thesis, University of São Paulo, 2004.
[24] G. C. S. C. Marques. Estudo e desenvolvimento de código computacional baseado no método dos elementos finitos para análise dinâmica não linear geométrica de sólidos bidimensionais. MS dissertation, University of São Paulo, 2006.
[25] D. N. Maciel. Análise de problemas elásticos não-lineares geométricos empregando o método dos elementos finitos posicional. PhD thesis, University of São Paulo, 2008.